A Cryo-CMOS PLL for Quantum Computing Applications

Gong, Jiang; Charbon, Edoardo; Sebastiano, Fabio; Babaie, Masoud

DOI
10.1109/JSSC.2022.3223629

Publication date
2023

Document Version
Final published version

Published in
IEEE Journal of Solid-State Circuits

Water Research 238 (2023) 120025

Contents lists available at ScienceDirect

Water Research

journal homepage: www.elsevier.com/locate/watres

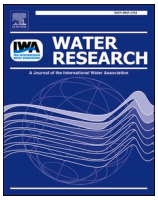

Highly efficient carbon assimilation and nitrogen/phosphorus removal facilitated by photosynthetic O_2 from algal-bacterial aerobic granular sludge under controlled DO/pH operation

Zejiao Li [a,1], Jixiang Wang [a,1], Jialin Liu [a], Xingyu Chen [a], Zhongfang Lei [a,*], Tian Yuan [a], Kazuya Shimizu [a,b], Zhenya Zhang [a], Duu-Jong Lee [c,d], Yuemei Lin [e], Yasuhisa Adachi [a], Mark C. M. van Loosdrecht [e]

[a] Faculty of Life and Environmental Sciences, University of Tsukuba, 1-1-1 Tennodai, Tsukuba, Ibaraki 305-8572, Japan
[b] Faculty of Life Sciences, Toyo University, 1-1-1 Izumino, Oura-gun Itakura, Gunma 374-0193, Japan
[c] Department of Mechanical Engineering, City University of Hong Kong, Kowloon Tang, Hong Kong
[d] Department of Chemical Engineering and Materials Science, Yuan Ze University, Chung-Li 32003Taiwan
[e] Department of Biotechnology, Delft University of Technology, van der Maasweg 9, HZ, Delft 2629, the Netherlands

ARTICLE INFO

Keywords:
Algal-bacterial aerobic granular sludge
Carbon fixation
Nitrogen assimilation
Photosynthetic oxygen
Simultaneous nitrogen and phosphorus removal

ABSTRACT

Reducing CO_2 emission and energy consumption is crucial for the sustainable management of wastewater treatment plants (WWTPs). In this study, an algal-bacterial aerobic granular sludge (AGS) system was developed for efficient carbon (C) assimilation and nitrogen (N)/phosphorus (P) removal without the need for mechanical aeration. The photosynthetic O_2 production by phototrophic organisms maintained the dissolved oxygen (DO) level at 3-4 mg/L in the bulk liquid, and an LED light control system reduced 10–30% of light energy consumption. Results showed that the biomass assimilated 52% of input dissolved total carbon (DTC), and the produced O_2 simultaneously facilitated aerobic nitrification and P uptake with the coexisting phototrophs serving as a C fixer and O_2 supplier. This resulted in a stably high total N removal of 81 ± 7% and an N assimilation rate of 7.55 mg/(g-MLVSS•d) with enhanced microbial assimilation and simultaneous nitrification/denitrification. Good P removal of 92–98% was maintained during the test period at a molar ΔP/ΔC ratio of 0.36 ± 0.03 and high P release and uptake rates of 10.84 ± 0.41 and 7.18 ± 0.24 mg/(g-MLVSS•h), respectively. Photosynthetic O_2 was more advantageous for N and P removal than mechanical aeration. This proposed system can contribute to a better design and sustainable operation of WWTPs using algal-bacterial AGS.

1. Introduction

The global wastewater generation is estimated at 359.4 billion m^3 annually, with only 53% receiving adequate treatment (Jones et al., 2021). The substantial volume of wastewater production and its associated environmental impacts drive the need for sustainable development of wastewater treatment plants (WWTPs). Aeration is these plants' most energy-intensive treatment unit, with energy consumption ranging between 0.27 and 1.89 kWh/m^3 in conventional activated sludge (CAS)-based WWTPs (Vergara-Araya et al., 2021). Additionally, WWTPs have been identified as a significant contributor to greenhouse gasses (GHGs) emission, mainly CO_2 from electricity consumption and biological processes (Campos et al., 2016; Larsen, 2015). As a result, reducing CO_2 emission and energy consumption in WWTPs has become a subject of increased attention.

Bacterial aerobic granular sludge (AGS) has become a popular option for wastewater treatment because of its compact structure, efficient settling, and high biomass retention, which can reduce operating costs and energy consumption (de Sousa Rollemberg et al., 2018). It has been applied in over 90 WWTPs in 20 countries (Nereda, 2023). However, it is worth noting that the application of AGS does not necessarily reduce CO_2 emission from biological processes. Additionally, sequencing batch

* Corresponding author.
E-mail address: lei.zhongfang.gu@u.tsukuba.ac.jp (Z. Lei).
[1] These authors contributed equally to this work.

https://doi.org/10.1016/j.watres.2023.120025
Received 27 January 2023; Received in revised form 26 April 2023; Accepted 29 April 2023
Available online 1 May 2023

reactors (SBRs) commonly used for AGS cultivation and operation (Adav et al., 2008; de Sousa Rollemberg et al., 2018) can contribute to a higher direct CO_2 emission compared to other processes, such as anaerobic/anoxic/oxic (A^2/O), anoxic/oxic (A/O), and oxidation ditch (Bao et al., 2015).

Cultivation of phototrophic organisms (including microalgae and cyanobacteria) using wastewater can provide a promising way to fix carbon (C) in WWTPs. Phototrophic organisms can fix CO_2 and produce high value-added biomass during the biological processes, reducing net CO_2 emission; simultaneously, the photosynthetic O_2 can help microbes decompose organics, remove nutrients, and substantially reduce electricity consumption required by aeration in biological WWTPs (Gonçalves et al., 2017; Muñoz and Guieysse, 2006). Unlike the big granule size of AGS, the tiny structure of phototrophic organisms (especially microalgae) leads to a low biomass settleability and a high energy requirement for biomass separation and harvesting (Gonçalves et al., 2017; Wang Q. et al., 2020). In addition, the cultivation of phototrophic organisms for nutrients removal requires a long hydraulic retention time (HRT) of 2–6 days (Muñoz and Guieysse, 2006), resulting in lower efficiencies when compared to nitrogen (N) removal by nitrifiers/denitrifiers and phosphorus (P) removal by polyphosphate-accumulating organisms (PAOs) in conventional biological WWTPs. More recently, the newly developed algal-bacterial AGS has attracted much attention due to its great potential for reduction in CO_2 emission and energy consumption since it combines the excellent properties of microalgae and/or phototrophic organisms and bacterial AGS (Abouhend et al., 2018; Ji et al., 2020a; Wang J. et al., 2020; Zhao et al., 2018). At its early stage, the algal-bacterial AGS were developed in SBRs with mechanical aeration (Huang et al., 2015; Liu et al., 2017), beneficial for granulation and stable granules maintenance. Nevertheless, the stripping effect of bubbling aeration operation may remove the inorganic C available for microalgae growth and the photosynthetic O_2 for aerobic bacteria (Li et al., 2022; Zhang et al., 2020). Therefore, the open airlift reactors may not fulfill this new granule system's and coexisting microalgae's potential. Currently, several studies have attempted to develop aeration-free algal-bacterial AGS systems where phototrophs fix inorganic C to produce O_2 for organics and nutrient removal, targeting the maximum effects of phototrophic organisms on C fixation and energy saving. Zhao et al. (2019) detected excellent C/N removal performance by the algal-bacterial AGS in shaking photo-reactors without mechanical aeration. Wang J. et al. (2020) achieved efficient C/P removal from a photosynthetic O_2-supported and closed photo-SBR with algal-bacterial AGS naturally developed from bacterial AGS. Ji and co-workers investigated N/P removal pathways in the algal-bacterial AGS system under non-aeration using successive cycle tests (Ji et al., 2020a, 2020b); they attributed the main N/P removal mechanisms to microbial assimilation. These previous works show that the activities of functional bacteria (including (de)nitrifiers and PAOs) are weakened in this aeration-free granule system. de Sousa Rollemberg et al. (2018) pointed out that functional bacteria can maintain highly efficient nutrient removal performance and play critical roles in granules formation and stability. Thus, good coordination between microalgae/phototrophs and functional bacteria can favor the sustainable operation and maintenance (O&M) of algal-bacterial AGS systems. Abouhend et al. (2018) noticed photosynthetic O_2-supported nitrification in an algal-bacterial AGS system treating the primary effluent from a WWTP under aeration-free conditions, in which efficient N removal was realized via nitrification and denitrification. However, little information is available on the sufficiency of photosynthetic O_2 to facilitate PAOs for P removal or both nitrifiers and PAOs, targeting stably high nutrient removal efficiency.

In the photosynthetic O_2-supported algal-bacterial AGS system, the growth of phototrophs can impact two critical parameters, namely dissolved oxygen (DO) concentration and pH, that are closely associated with the activities of functional bacteria under uncontrolled conditions. Therefore, this study was designed to coordinate microalgae/phototrophs with functional bacteria for simultaneously high efficiencies of N/P removals and C fixation in algal-bacterial AGS by adopting the following strategies: (1) pH control for enhanced growth of the functional bacteria; (2) DO control to eliminate adverse impacts of high DO concentration on phototrophs and functional bacteria for reduced light energy consumption; and (3) a shorter oxic phase to promote simultaneous nitrification and denitrification for improved N removal and reduced energy consumption. In this study, batch cycle tests, mass balance analysis, and microbial communities analysis were also conducted to shed light on the mechanisms involved in C/N/P removal and the C and O_2 mass exchanges between microalgae/phototrophs and bacteria.

2. Materials and methods

2.1. Experimental setup of photo-SBR

The experimental photo-SBR was a glass beaker (AS ONE, Japan) with a working volume of 1.0 L (10.4 cm in inner diameter and 15.1 cm in height). Two LED lights (NLSS20C, NIKKI, Japan) were placed opposite at the right and left sides to provide a photon flux density of about 480 μmol s^{-1} m^{-2} (about 28 klx) at the beaker wall. An overhead stirrer (OS20-S, DLAB, China) was operated at 150 rpm to ensure the mature granules in suspension in the beaker during the anaerobic and oxic phases. A pH controller (NPH-6900, Nissin Rika, Japan) was used to monitor and control the bulk pH by automatically adding 0.5 mol/L HCl when the bulk pH rose above the setpoint pH. The bulk DO concentration was also monitored and/or controlled by a DO controller (HI8410, Hanna Instruments, USA) connected to the two LED lights that were automatically switched on or off at the DO level below or above the set range.

2.2. Operation of the photo-SBR

In a pre-experiment, the impact of atmospheric O_2 on aerobic P uptake and nitrification was evaluated using this open photo-SBR under the same operating conditions described in Section 2.1. The DO concentration remained below 0.1 mg/L after a one-hour anaerobic phase. The concentrations of P and NH_4^+-N were detected almost unchanged during a subsequent three-hour test period under no illumination and mechanical aeration (air bubbling). These results indicate that atmospheric O_2 had minimal influence on this open system under the operational conditions applied.

As shown in Table 1, the whole study comprised three Stages. During Stage I, according to the nutrient removal profiles from a pre-experiment, the open photo-SBR was operated at a 4-h cycle consisting of 50 min anaerobic phase (including 5 min feeding), 170 min illumination phase (oxic phase), 3 min settling, 5 min discharging, and 12 min idling. Among them, anaerobic, oxic, and idling durations were set to allow completely anaerobic P release, aerobic NH_4^+-N and P removal, and residual O_2 removal, respectively. The bulk pH was controlled at $\leq$ 8.0 during the illumination period, facilitating the

Table 1
Experimental conditions during the three test stages.

	Duration	pH control	DO control (mg/L)	Cycle time (h)	Hydraulic Retention Time (HRT, h)
Stage I	Days 1 ~ 7 (7 d)	≤ 8.0	No control	4	8
Stage II	Days 8 ~ 13 (6 d)	≤ 8.0	3 ~ 4*	4	8
Stage III	Days 14 ~ 43 (30 d)	≤ 8.0	3 ~ 4*	3	6

* The DO concentration may be a little bit lower than 3 mg/L during the increase period of DO by photosynthetic O_2 production due to the delayed response of the DO controller. Solids retention time (SRT) was not controlled during the test periods.

activities of PAOs and nitrifiers (Li et al., 2022). DO was monitored but not controlled during Stage I, and the volumetric exchange ratio (VER) was controlled at 50% (HRT=8 h). During Stage II, a feedback loop "Phototrophs → Light → O_2 → DO controller → Light → Phototrophs" was constructed through the DO controller to stabilize the growth of phototrophic organisms and reduce input illumination/energy consumption. The LED lights were switched on via the DO controller at DO < 3 mg/L, which were switched off at DO > 4 mg/L during the illumination phase. During Stage III, under the controlled bulk pH and DO concentration conditions, the cycle time was optimized for a higher wastewater treatment efficiency and capacity, in which the oxic and idling periods were decreased to 115 min and 7 min, respectively, leading to a shorter cycle time of 3 h (HRT = 6 h) with the other operational parameters being unchanged. The solid retention time (SRT) was not controlled in this study, estimated as 28, 10, or 14 days during Stages I, II, or III, respectively, according to the discharged effluent biomass and sampled sludge for analysis (averagely 10 mL/d). It was worth mentioning that the operation of algal-bacterial AGS was not stopped after the experiments in this study because this proposed system was then used to examine other impact factors and some interesting phenomena to better its design and sustainable operation.

The seed algal-bacterial AGS was sampled from a mother photo-SBR treating synthetic domestic wastewater, which has been stably operated for 3 years in the laboratory. The synthetic wastewater (pH ~ 7.4) was prepared with tap water and chemicals as previously (Wang et al., 2021). During the whole test period, the average concentrations of the primary influent nutrients and ions were as follows: Dissolved organic carbon (DOC, with CH_3COONa as the sole organic carbon), 91.05 ± 4.22 mg/L; dissolved inorganic carbon (DIC), 27.19 ± 1.65 mg/L; total P (TP, KH_2PO_4), 4.77 ± 0.18 mg/L; total N (TN, NH_4Cl), 30.57 ± 1.63 mg/L; K^+, 11.74 ± 1.09 mg/L; Mg^{2+}, 11.43 ± 0.36 mg/L; Ca^{2+}, 22.89 ± 0.69 mg/L; Na^+, 158.30 ± 5.00 mg/L; Cl^-, 131.59 ± 7.13 mg/L; SO_4^{2-}, 50.25 ± 1.22 mg/L; and Fe^{2+}, 0.24 ± 0.02 mg/L.

2.3. Cycle and batch tests

2.3.1. General cycle tests

During the test period, two consecutive cycle tests were performed every 2 – 4 days to check the reactor performance, with average values being reported. In addition, a 1:1 (v/v) mixture solution of influent (synthetic wastewater) and effluent from the previous cycle was used as the sample at zero min during the cycle tests.

2.3.2. Batch tests

In the batch tests, aeration, instead of photosynthetic O_2 to maintain DO concentration at 3 - 4 mg/L, was performed to illuminate the role of phototrophic organisms. The lights were switched off during the oxic phase, but an air pump aerated the bulk liquor at a low aeration rate of 0.3 L/min. Other parameters, including stirring, were the same as the cycle tests in Section 2.3.1.

2.3.3. Mass balance analysis of C, N, and P

In order to analyze the fates of influent C, N, and P, mass balance analysis was performed during the stable operation from days 31 to 43. During this period, the sampled effluents were centrifuged. The liquid was used to analyze soluble C/N/P concentrations, and the solid was collected and stored at -18 °C for further quantification of C/N/P contents in the effluent biomass. In addition, the granular C/N/P contents were also quantified from the sampled granules. The released C and N were calculated by subtracting C and N in the liquid and solid portions from the total input C and N amounts.

2.4. Calculations and statistical analysis

2.4.1. Calculations

The calculations of (1) total emitted C or N (mg/(g-MLVSS•d)) and assimilated C or N in biomass (mg/(g-MLVSS•d)), (2) the molar ratios of ΔP/ΔC, ΔK/ΔP, ΔMg/ΔP, or ΔCa/ΔP for estimation of PAOs activity (Acevedo et al., 2012), (3) P release or uptake rates (mg/(g-MLVSS•h)), and (4) nitrification efficiency (%) were described in detail in the Supplementary Material.

2.4.2. Statistical analysis

Paired- samples T-Test was adopted to analyze the statistical difference of datum using IBM SPSS Statistics 27. $p < 0.05$ was assumed as statistically significant difference. The linear correction coefficient was also calculated.

2.5. Analytical methods

Mixed liquor (volatile) suspended solids (ML(V)SS) were determined according to the standard methods (APHA, 2012). The pigment contents, including chlorophyll-*a*, (Chl-*a*), chlorophyll-*b* (Chl-*b*), and carotenoids, were extracted by using the methanol method and quantified according to Pancha et al. (2014). The concentrations of acetate, PO_4^{3-}, NO_2^- and NO_3^-, Cl^-, Na^+, NH_4^+, K^+, Mg^{2+}, and Ca^{2+} in the liquid were quantified by Ion Chromatography (SHIMADZU, Japan) after samples being filtered through 0.22 μm membrane filters (Wang et al., 2021). Total P and N in liquid were measured with the standard methods (APHA, 2012) after the samples were completely oxidized with persulfate. Dissolved total carbon (DTC), solid TC, dissolved inorganic carbon (DIC), and dissolved organic carbon (DOC) in the liquid were measured by the TOC detector (TOC-VCSN, SHIMADZU, Japan) equipped with an autosampler (ASI-V, SHIMADZU, Japan) and a solid sample combustion unit (SSM-5000A, SHIMADZU, Japan). The total N (TN) in solid was determined by an elemental analyzer (UNICUBE, Elementar, Germany). The extraction and determination of total phosphorus (TP), apatite phosphorus (AP), and non-apatite inorganic phosphorus (NAIP) were performed according to a previous study (Wang et al., 2021). The extracellular polymeric substances (EPS) were quantified after being extracted from the mixed suspended granules with a heating method following the same procedures (Wang et al., 2021): after being crushed and centrifuged, the liquid was used for the analysis of loosely bound EPS, and the residual sludge was re-suspended and treated at 80 °C for 30 min for quantification of tightly bound EPS. Granular morphology and size were recorded by microscope (Leica M205 C, Leica Microsystems, Switzerland) and analyzed by ImageJ 1.53a.

The Lab-Aid824s DNA Extraction kit (ZEESAN) extracted total DNA from freeze-dried sludge samples. A 2-step tailed PCR method was used to amplify 16S rRNA and 18S rRNA gene fragments from the extracted DNA using primers of 338F/806R and 1422f/1642r, respectively. The verified amplicons were subjected to paired-end sequencing on the Illumina MiSeq sequencing platform at Bioengineering Lab Co. Ltd. (Japan). The raw reads have been deposited in the NCBI Sequence Read Archive (SRA) database (Accession Number: PRJNA957041).

3. Results and discussion

3.1. Changes in granule properties

3.1.1. Biomass concentration, pigments, and EPS

The results shown in Fig. 1A indicate a rapid increase in MLVSS from 5.1 ± 0.1 g/L on day 1 to 7.1 ± 0.1 g/L on day 7 during Stage I, accompanied by a corresponding increase in Chl-*a* content from 5.3 ± 0.1 to 7.4 ± 0.5 mg/g-MLVSS (Fig. 1B). During Stage II, however, the MLVSS decreased to 5.1 ± 0.4 g/L (Fig. 1A). In contrast, the Chl-*a* content continued to increase to 12.0 ± 0.4 mg/g-MLVSS on day 13 (Fig. 1B), probably due to high effluent biomass and decreased inhibition of controlled DO on the growth of phototrophic organisms. In Stage III, both MLSS and MLVSS showed an upward trend, while the effluent biomass decreased and then remained stable, achieving a biomass yield of about 0.64 g-MLVSS/g-COD during the last 12 days. Despite the

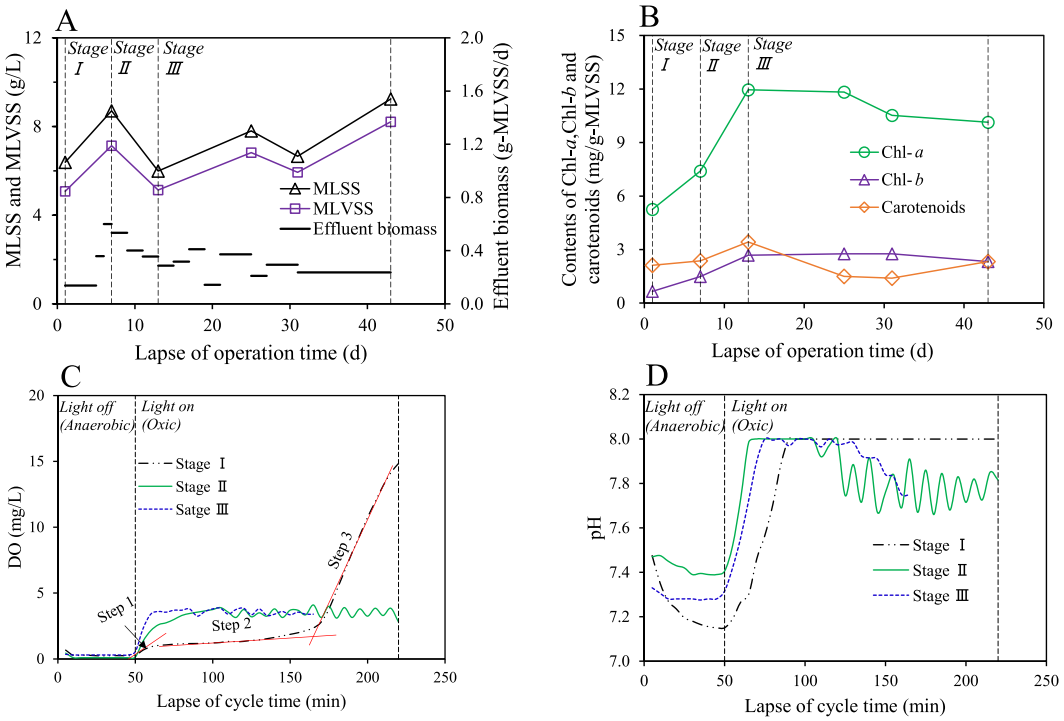

Fig. 1. Variations of biomass concentration (A) and pigments content (B) during the three operational stages; Profiles of typical DO (C) and pH (D) in the cycle tests during the three operational stages.

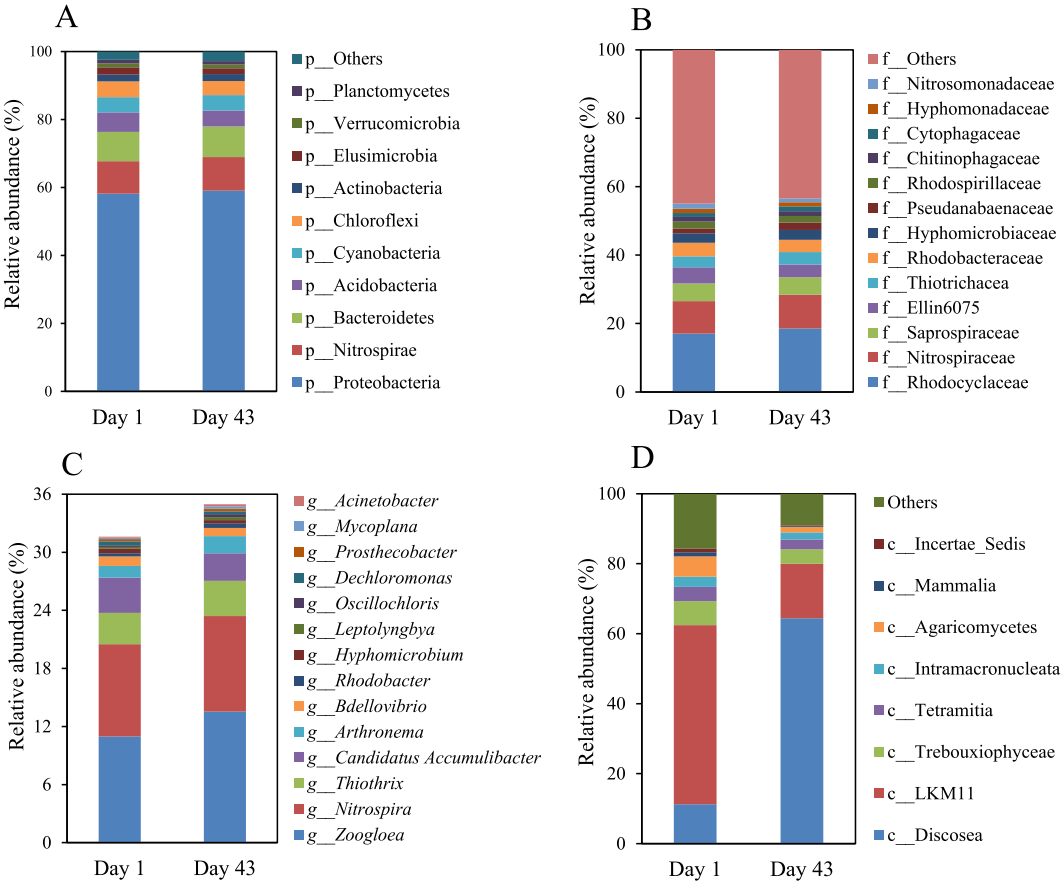

Fig. 2. Changes in microbial communities including prokaryotes at phylum (> 1%, A), family (> 1%, B), and genus (top 14 identified groups, C) levels in addition to eukaryotes (D) in the algal-bacterial aerobic granular sludge AGS on day 1 and day 43, respectively.

reduced illumination time as a result of the shortened cycle time and controlled DO, a high Chl-*a* content of 11.1 ± 0.9 mg/g-MLVSS was maintained (Fig. 1B). This content is significantly higher than those of algal-bacterial AGS developed under mechanical aeration conditions (He et al., 2018a; Wang et al., 2022), but close to those of algal-bacterial AGS developed under non-aeration conditions (Ji and Liu, 2022; Wang J. et al., 2020; Zhao et al., 2019). Additionally, the trend in Chl-*b* content was similar to that of Chl-*a* (Fig. 1B), while the carotenoid content showed a slight increase during Stages I and II and decreased during Stage III (Fig. 1B). This observation may suggest no photoinhibition to phototrophic organisms in this system, as a high carotenoid content with low Chl-*a* content is generally considered a sign of photoinhibition (Sousa et al., 2013). The variation of EPS and their components, polysaccharides (PS) and proteins (PN), are associated with the changes in granular stability. Both PS and PN contents decreased during Stage I. However, they gradually increased during Stage II (Fig. S1), which may imply that the granular stability deteriorated to some extent during Stage I while recovered during Stage II, in agreement with the variations of effluent biomass concentration (Fig. 1A).

3.1.2. Granule morphology

The seed algal-bacterial AGS was nearly spherical with a compact structure and smooth surface, entangled with green microalgae and surrounded by some filamentous organisms (Fig. S2). The average diameter of seed granules was 1.24 ± 0.59 mm, and about 44% were smaller than 1.00 mm. Along with the operation, the granules became more brushy with more significant amounts of green matter, which was also indicated by the increment of Chl-*a* content. On day 31, some brown matter appeared and intertwined with the filamentous organisms, which promoted the growth of some small new granules, increasing the percentage of granules with a diameter of < 1.00 mm. The newly grown granules were cylindrical, different from the spherical granules sampled from the mother photo-SBR, probably due to the stirring operation.

3.1.3. Microbial community

Fig. 2 shows that the relative abundances of major functional bacteria kept well during the test period in this photo-SBR. Nitrosomonadaceae (1 - 2%) and Nitrospiraceae (9 - 10%), the frequently reported ammonia-oxidizing bacteria (AOB) and nitrite-oxidizing bacteria (NOB) (He et al., 2018b), remained relatively stable during the entire period, suggesting a stable nitrification process. The genera *Paracoccus* and *Pseudomonas* as typical denitrifying bacteria were detected but presented a low relative abundance of < 0.04% in this system, thus the enriched *Zoogloea* and *Acinetobacter* possibly contributed to denitrification (Rajta et al., 2020). The typical PAOs like the genus *Candidatus Accumulibacter* (Oehmen et al., 2007) were also detected at a relative abundance of 3 - 4%. These data imply the stable nutrient removal performance by the functional bacteria.

The identified eukaryotic microalgae were class Trebouxiophyceae, but their relative abundance decreased from 7% on day 1 to 4% on day 43 (Fig. 2D). Thus, the increased Chl-*a*/*b* and carotenoid contents (Fig. 1B) were probably attributable to the growth of photosynthetic bacteria, including genera *Arthronema, Leptolyngbya, Rhodobacter*, and *Oscillochloris* (Fig. 2C). Besides the genera *Arthronema* and *Leptolyngbya* of Cyanobacteria, the genus *Thiothrix* of Proteobacteria possibly contributed to the filamentous structure of algal-bacterial granules.

3.2. Changes of DO and pH, and their control strategies

During the operation of Stage I, a significant amount of photosynthetic O_2 production was detected during the illumination phase (Figs. 1C and S3A), which is sufficient for both aerobic P uptake and nitrification. The DO profile was characterized as three steps during the light-on period of Stage I: (1) DO concentration rapidly rose after initializing the illumination (Step 1); (2) DO reached a stable concentration (Step 2), during which the generated O_2 was consumed by aerobic P uptake, nitrification and/or other aerobic reactions as discussed in Sections 3.4 and 3.5 (Please note that the DO concentration was elevated by 1–3 mg/L along with the operation (Fig. S3A), possibly resulting from the increased Chl-*a* content); and (3) at Step 3, the DO concentration linearly increased to a level up to supersaturation. In this step, the photosynthetic O_2 was much more than the O_2 consumption needed by the system. Such a too-high DO concentration may affect P uptake by PAOs (Carvalheira et al., 2014) and N removal by denitrifiers (Mosquera-Corral et al., 2005). Thus the DO concentration in the subsequent oxic phases during Stages II and III was controlled at 3 - 4 mg/L via the DO controller and LED lights on/off, which was set slightly higher than the stable DO concentration (Step 2) at the end of Stage I, as a higher DO concentration may allow phototrophic organisms to fix more inorganic C. During Stages II and III, the DO concentration increased faster to the set DO range (3 - 4 mg/L) in Step 1 (Fig. S3A) than in Stage I due to their higher Chl-*a* contents. With adequate DO control, some balance might be established among Chl-*a* content, DO concentration, and illumination. As such, the increased Chl-*a* content promotes photosynthetic O_2 production to increase DO; the rapid increase of DO activates the DO controller to switch off the LED lights, limiting the phototrophs growth (increase in Chl-*a* content). This resulted in a relatively stable Chl-*a* content during Stage III (Fig. 1B).

During the anaerobic phase, the pH slightly decreased (Fig. 1D), probably due to the combined effects of influent wastewater and anaerobic decomposition. Once the illumination was initiated, the pH linearly rose to the controlling point of 8.0 due to CO_2 consumption by photosynthesis. During Stages I and II, the time needed for pH rising to the setpoint (pH 8.0) were gradually shortened (Fig. 1D), owing to the increased phototrophs growth indicated by Chl-*a* content. During Stage III, the principal pH rise was completed in 30 min, attributable to the granules' relatively stable and high Chl-*a* content (Fig. 1B and D). Then the pH gradually decreased with DO fluctuations after reaching the set DO. In this proposed system, the illumination phase is dominated by three biological reactions: photosynthesis by phototrophs, aerobic P removal by PAOs, and (de)nitrification by (de)nitrifiers, respectively (Fig. 2). For simplicity, microbial assimilation was not taken into consideration in these bioreactions. The following reactions (1–4) summarize the major biological processes as described by Gerardi (2002) and Smolders et al. (1995).

$$Photosynthesis: CO_2 + H_2O \rightarrow CH_2O + O_2 \quad (1)$$

$$P\ uptake: 0.87CH_{1.5}O_{0.5} + O_2 + 3.23\ H_3PO_4 \rightarrow 3.23HPO_3 + 0.87CO_2 + 3.87\ H_2O \quad (2)$$

$$Nitrification: 0.5NH_4^+ + O_2 \rightarrow 0.5NO_3^- + H^+ + 0.5H_2O \quad (3)$$

$$Denitrification: 0.625\ CH_2O + 0.5\ NO_3^- + 0.5\ H^+ \rightarrow 0.25\ N_2 + 0.625CO_2 + 0.875\ H_2O \quad (4)$$

P uptake and nitrification are pH-decreasing processes, while photosynthesis and denitrification are pH-increasing processes. Seen from the above reactions, one mmol CO_2 corresponds to one mmol O_2 production during photosynthesis; One mmol O_2 utilized by nitrifiers can generate one mmol H^+ or 0.87 mmol CO_2 by PAOs. If all the produced NO_3^- is denitrified, one mmol O_2 consumed would produce 0.50 mmol H^+ and 0.63 mmol CO_2. In this reaction, the contribution of produced protons is much more significant than CO_2, considering the very low dissociation constant of carbonic acid, $pK_{a1} = 6.37$ (25 °C). Therefore, the decrease in pH is mainly attributable to nitrogen removal during the illumination phase. Restated, in the present photo-SBR system, the increased pH by photosynthesis based on the unit O_2 produced was lower than the decreased pH by nutrient removal based on the unit O_2 utilized. As such, if the pH controller controlled the LED lights to maintain liquid pH, the DO increase by photosynthesis based on a unit pH elevated will be higher than the DO decrease by nutrients removal

based on a unit pH decreased, which has been supported by an increasing DO concentration during the oxic phase (data not shown).

3.3. C removal

3.3.1. Changes in C species and their removal

The photo-SBR system demonstrated an excellent and stable DOC removal efficiency of 90 ± 3% during the entire test period (Fig. 3A). The average effluent DOC was 8.95 ± 2.78 mg/L, close to the effluents from bacterial or algal-bacteria AGS systems (Zhao et al., 2018). This observation is attributable to the dissolved organic substances excreted by the coexisting microalgae and/or bacteria since the sole organic carbon (sodium acetate) was almost completely removed within the initial 30 min during the anaerobic phase (Figs. 3C and S4A). During Stages I and II, the effluent DIC concentration remained low at 17.44 ± 3.56 mg/L, lower than the influent DIC concentration. When the illumination duration was shortened during Stage III, the effluent DIC concentration slightly increased, very close to the influent DIC, suggesting less contribution of phototrophic organisms to the DIC removal.

Under the mechanical aeration operation, an insignificant increase of DIC was detected (Fig. 3D), in which DIC from acetate degradation may be stripped into the air by aeration operation. In the photosynthetic O_2 condition, the DIC concentration decreased during the illumination period (Fig. 3C), demonstrating the great potential of the algal-bacterial AGS system for GHGs emission reduction.

3.3.2. C assimilation and CO_2 emission reduction

As expected, the TC content in granules increased from 405.7 mg/g-MLVSS on day 1 to 460.3 mg/g-MLVSS on day 43. The average C assimilation rate was 35.03 mg/(g-MLVSS•d) during the last 12 days (Table 2). To estimate the contribution of phototrophs to C fixation in the algal-bacterial AGS, an empirically stoichiometric formula of $CH_{1.78}O_{0.36}N_{0.12}P_{0.01}$ (Boelee et al., 2014) for phototrophs and a ratio of 56.31 mg-MLVSS/mg-Chl-*a* (Samiotis et al., 2021) were used. As shown in Table 2, the contribution of phototrophic organisms to C sequestration was about 23.28 mg/(g-MLVSS•d), with a CO_2 fixation capacity of 85.36 mg-CO_2/(g-MLVSS•d), which accounted for about 66% of total C assimilation by the algal-bacterial AGS.

The CO_2 emission from this algal-bacterial granule system was only 0.25 kg-CO_2/kg-COD (without consideration of other direct and indirect CO_2 emissions), much lower than 0.58, 0.68, 0.76, and 0.97 kg-CO_2/kg-COD from the four full-scale A^2O, AO, oxidation ditch, and SBR-based WWTPs (Bao et al., 2015), indicating its great potential of reducing GHGs emission. It was estimated that 14% of input DTC was released, while the biomass assimilated 52% of input DTC. In this study, the contribution of phototrophic organisms to C fixation was limited due to the short illumination duration of 80 – 104 min under the DO control strategy applied. In order to achieve more reduction of CO_2 emission from this photo-SBR, the DO control range is a crucial factor which needs more in-depth studies.

3.4. N removal

3.4.1. N removal and nitrification efficiency

As shown in Fig. 4, effective N removal was achieved through the photosynthetic O_2 supply. The effluent TN concentrations rapidly decreased during Stage I and kept relatively stable during Stage II, possibly associated with the relatively low DO concentration compared to the near-saturated DO concentration in the mother photo-SBR. The effluent NO_3^--N concentration followed the trend of the effluent TN, while the effluent NH_4^+-N and NO_2^--N concentrations were negligible during these two stages. As a result, the TN removal efficiency was increased from 62% on day 1 to 79 ± 2% during Stage II, with NH_4^+-N removal of nearly 100% during Stages I and II.

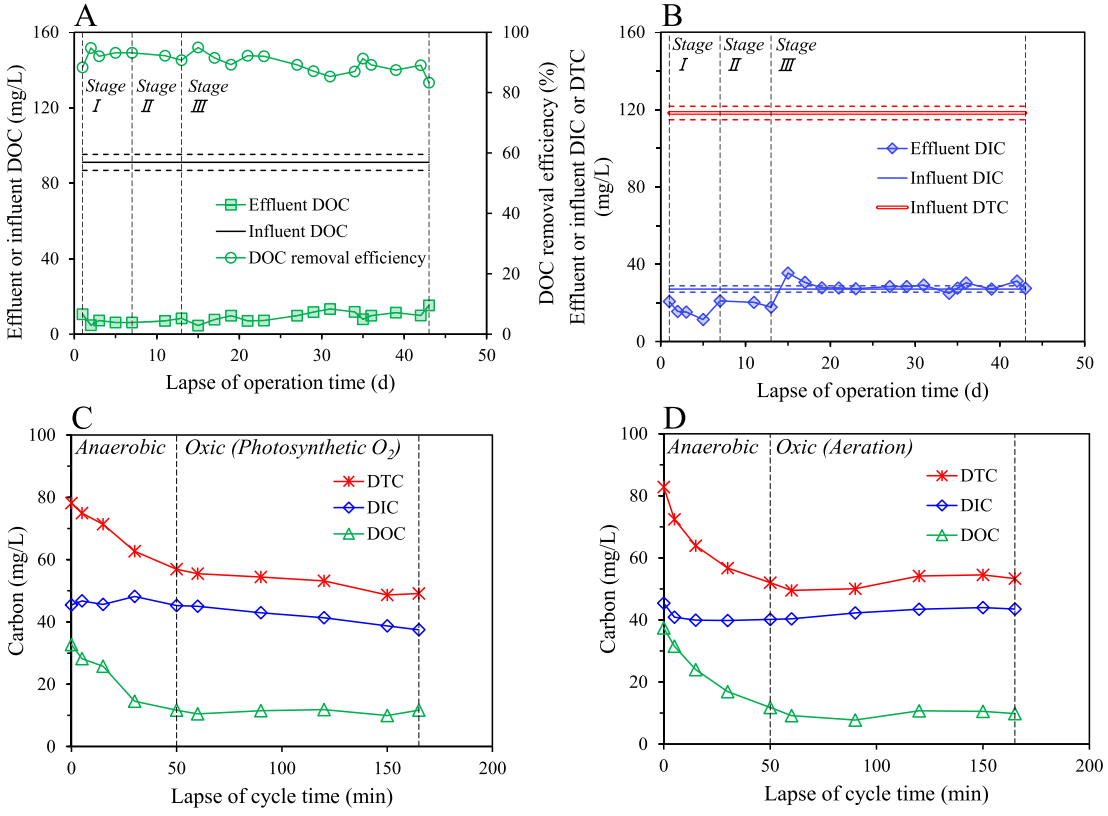

Fig. 3. Variations of DOC (A) and effluent DIC (B) concentrations during the three operational stages; and typical dissolved C profiles with the oxic phase maintained by the photosynthetic O_2 (C) and the mechanical aeration (D) in the batch tests.

Table 2
Mass balance analyses of total C, N, and P during the last 12 days' operation.

Element	Input		Assimilated in biomass			Effluent liquid	Emission[a]	Contribution of phototrophs[b]
	Total	Total organic	Grown	Discharged	Effluent			
C (mg/(g-MLVSS•d))	66.87	51.50	14.22	4.68	16.13	22.44	9.40	23.28
P (mg/(g-MLSS•d))	2.40	–	1.20	0.23	0.65	0.12	–	0.60
N (mg/(g-MLVSS•d))	17.29	–	3.22	0.90	3.43	2.50	7.24	3.26

[a] Calculated as ([Input] – [Fixed in biomass] – [Effluent liquid].
[b] Estimated according to an assumed stoichiometric formula ($CH_{1.78}O_{0.36}N_{0.12}P_{0.01}$) of microalgae (Boelee et al., 2014) and the ratio (54%) of microalgae's MLVSS to Chl-a (Samiotis et al., 2021).

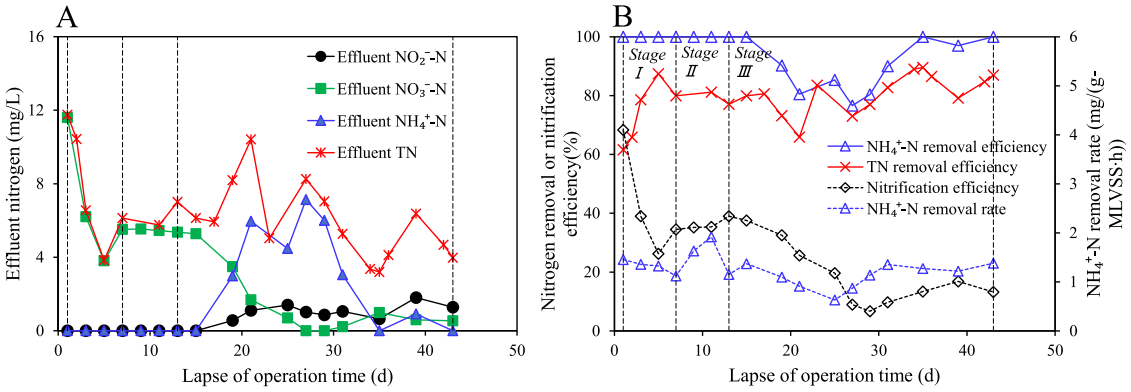

Fig. 4. Profiles of effluent nitrogen (A), nitrification efficiency, and nitrogen removal rate (B) during the three operational stages.

An interesting phenomenon was observed when the illumination duration was shortened during Stage III. The photo-SBR experienced a deterioration period and then recovery of N removal. The effluent NH_4^+-N concentration increased first and then decreased, while the effluent NO_3^--N concentration decreased first and remained low. In addition, the effluent NO_2^--N concentration slightly increased. As such, the NH_4^+-N removal efficiency dropped to 77% on day 27 and then recovered to nearly 100%, while TN removal efficiency kept at 81 ± 7% during Stage

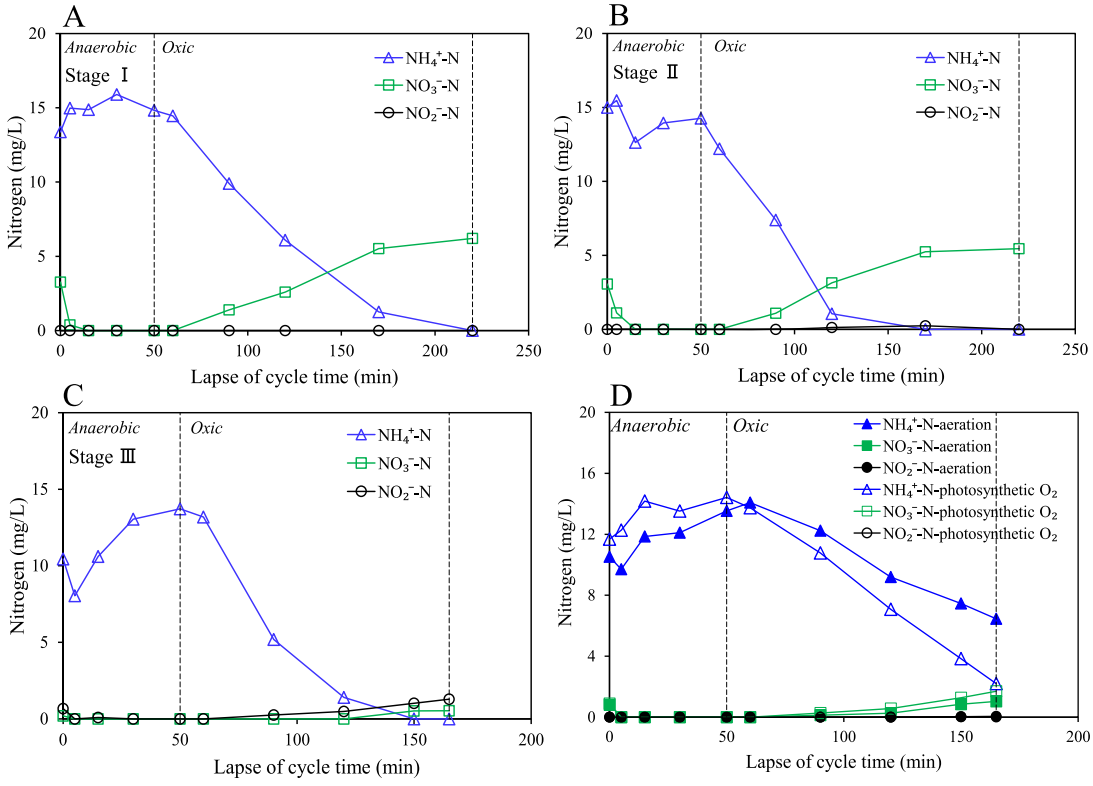

Fig. 5. Changes in N species during the cycle tests in Stages I (A), II (B), and III (C), and their comparative results from mechanical aeration and illumination conditions (D).

III.

A competitive NH_4^+-N removal rate was obtained during the entire test period (Fig. 3B), averagely 1.25 ± 0.30 mg/(g-MLVSS•h), much higher than 0.89 ± 0.05 mg/(g-MLVSS•h) of a bacterial AGS system under an aerobic/oxic/anoxic mode (He et al., 2016). On the other hand, the nitrification efficiency was almost halved from 68% to 35% during Stage I. It remained at 36 ± 2% and 20 ± 12%, respectively during Stages II and III, significantly lower than 80% by the mother photo-SBR. Considering the relatively stable TN removal efficiency, it can be inferred that more N might be emitted and/or assimilated in the biomass during the operation.

3.4.2. Main contributors to N removal

As illustrated in the cycle tests (Fig. 5A and B), NH_4^+-N removal was rapidly initiated once the LED lights switched on, while NO_3^--N was correspondingly produced during Stages I and II. In Stage I, N removal was completed in 2 h illumination, in correspondence with the stable DO concentration (Step 2 in Fig. 1C). The above results indicated a photosynthetic O_2 driving aerobic nitrification process, which was evidenced by the stable AOB and NOB abundance in granules (Fig. 2). On the other hand, the generated NO_3^--N and low NO_2^--N production cannot cover the decreased amount of NH_4^+-N. What is more, the effluent NO_3^--N decreased with the operation. Such an increasing N loss may imply its complex N removal pathways including microbial assimilation, simultaneous nitrification and denitrification, anammox, and/or ammonia precipitation (such as struvite formation).

The TN content in the seed granules was about 92.0 mg/g-MLVSS, higher than 56.7 ± 11.3 mg/g in the activated sludge (Chen et al., 2021) used for the initial seed sludge for granulation in the mother photo-SBR. In addition, the granular N content did not increase with the increase in Chl-*a* content, which was about 88.4 mg/g-MLVSS on day 31 and 91.4 mg/g-MLVSS on day 43. According to the N balance analysis (Table 2), approximately 44% of input N was assimilated in biomass compared to the maximum 20% by seed granules in the mother photo-SBR from their nitrification efficiency. This significant difference is attributable to the enhanced assimilation by phototrophic bacteria indicated by the increased Chl-*a* content (Fig. 1B) and enriched *Arthronema, Leptolyngbya, Rhodobacter,* and *Oscillochloris* (Fig. 2C). The N assimilation rate was about 7.55 mg-N/(g-MLVSS•d) in this study, lower than 11–37 mg-N/(g-MLVSS•d) by activated sludge with enriched nitrogen-fixing bacteria treating thermomechanical pulping wastewater (Slade et al., 2003). The N assimilation rate of phototrophs was estimated as 3.26 mg-N/(g-MLVSS•d) (Table 2), indicating that bacteria in this system contributed about half of N assimilation. As illustrated in Fig. 5D, the photosynthetic O_2 can help remove N faster with a higher N removal efficiency when compared to the mechanical aeration, suggesting less contribution of nitrifiers to N removal in this algal-bacterial AGS system. However, a similar nitrification efficiency of 14% was observed under the two O_2 supply strategies, implying that the N species assimilated by phototrophs include both NH_4^+-N and NO_3^--N since whichever N species was utilized alone by phototrophs would contribute to their difference in nitrification efficiency (Fig. 5D).

Simultaneous nitrification and denitrification are considered other competitive contributors to N removal since about 42% of input N was emitted from the system according to the N balance analysis. Although a low NO_2^--N and NO_3^--N during NH_4^+-N removal process may imply the possibility of shortcut denitrification during Stage III, the enriched Nitrospiraceae directly indicated a stable nitrite-oxidizing process. Therefore, shortcut denitrification is not considered a major N emission pathway. The low DO concentration, increasing granular size (Fig. S2), and short oxic time may favor denitrification in the AGS systems (Abouhend et al., 2023; He et al., 2018b; Mosquera-Corral et al., 2005) probably accounting for simultaneous nitrification and denitrification in the present system. On the other hand, the DOC concentrations during the illumination phase were statistically ($p < 0.05$) higher than those under the mechanical aeration condition (Fig. 3C and D), which may be utilized as carbon sources to some extent. Thus, the relatively high phototroph content and the photosynthetically produced DOC or organic matter may favor simultaneous nitrification and denitrification.

It is worth mentioning that the removal of NH_4^+-N by ammonia precipitation (struvite) was excluded since struvite is unsaturated under the low pH value ≤ 8.0 estimated by Visual MINTEQ 3.1 software. On the other hand, during the NH_4^+-N removal process, the set DO range of 3 - 4 mg/L still maintained an oxic condition with almost no NO_2^- accumulation (Fig. 5). In addition, the typical anammox bacteria, such as genera *Brocadia, Kuenenia, Anammoxoglobus, Jettenia,* and *Scalindua,* were not detected in the granules (Fig. 2). The anammox process is thus not considered as the primary N removal pathway in this study.

3.5. P removal

3.5.1. P removal efficiency and removal rate

A highly efficient P removal was achieved through photosynthetic O_2 production that supports aerobic P uptake. During Stage I, the TP removal efficiency rapidly increased from 42% on day 1 to 98% on day 7 (Fig. 6A), indicating that the algal-bacterial AGS quickly adapted to the new environment under the adopted pH control strategy. The controlled DO and shortened illumination time also showed little adverse impact on TP removal efficiency, which remained at 97 ± 2% and 92 ± 8% during Stages II and III, respectively.

The P release and uptake functioned well during the test period (Fig. 6B and Fig. S4B). The P uptake process was completed within 2 h illumination during Stages II and III, corresponding to the stable DO concentration (Step 2 in Fig. 1C); during this period, the O_2 generated by phototrophic organisms was used for aerobic P uptake and nitrification. The P release rate of the seed granules was about 27.57 mg/(g-MLVSS•h), much higher than 2.87 ± 0.29 mg/(g-MLSS•h) from the bacterial AGS (He et al., 2016) and 16.24 ± 0.91 mg/(g-MLVSS•h) from the algal-bacterial AGS system under no pH control (Li et al., 2022). During Stage I, the P release rate decreased quickly to 16.55 mg/(g-MLVSS•h) on day 7, accompanied by the decrease of maximum P release; this decreasing trend continued during Stage II with a lower decrease rate till day 25 (Fig. 6B). Finally, the P release rate remained around 10.84 ± 0.41 mg/(g-MLVSS•h) during the subsequent operation. During Stages I and II, the growth of phototrophic bacteria and higher effluent biomass (Figs. 1A and 2) possibly led to the low granular polyP content that accounts for the decrease in P release rate. This deduction is partially evidenced by the decrease in granular NAIP content (Fig. 7D). In contrast, the variation of P uptake rate was insignificant, averagely 7.18 ± 0.24 mg/(g-MLVSS•h) during the entire test period. Li et al. (2022) pointed out that aerobic P uptake is limited by intra-particle diffusion, including macropore and micropore diffusion in the algal-bacterial AGS. Luo et al. (2014) claimed that flocculent sludge had a higher surface area than AGS. According to the morphological changes of the algal-bacterial AGS (Fig. S2), the granules became more significant with more filamentous matter attached along with the operation. This morphological change may increase granular surface area and improve intra-particle diffusion limitation, maintaining the stable granular P uptake rate under the controlled DO/pH operation conditions.

3.5.2. P removal pathway

All the plots of ΔP against ΔC achieved high linear correlation coefficients (R^2) (Fig. 7A). Similar to the changes in P release rate, the molar ΔP/ΔC ratio significantly decreased during Stages I and II, implying the decreased PAOs activity in the granules (Acevedo et al., 2012). During Stage III, the molar ΔP/ΔC ratio was 0.36 ± 0.03, lower than 0.48–0.80 for PAOs-enriched cultures but much higher than 0 - 0.02 for GAOs-enriched cultures (Acevedo et al., 2012). Meanwhile, the genus *Candidatus Accumulibacter* of PAOs slightly decreased from 4% on day 1 to 3% on day 43 (Fig. 2). This observation suggests that the PAOs primarily contributing to P removal were still active in the present study.

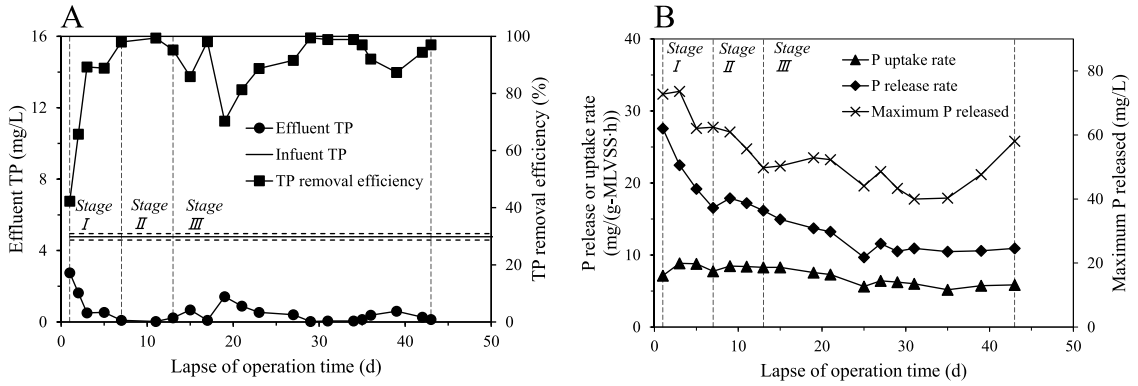

Fig. 6. Changes in effluent TP concentration and TP removal efficiency (A), and P release and uptake rates during the three operational stages (B).

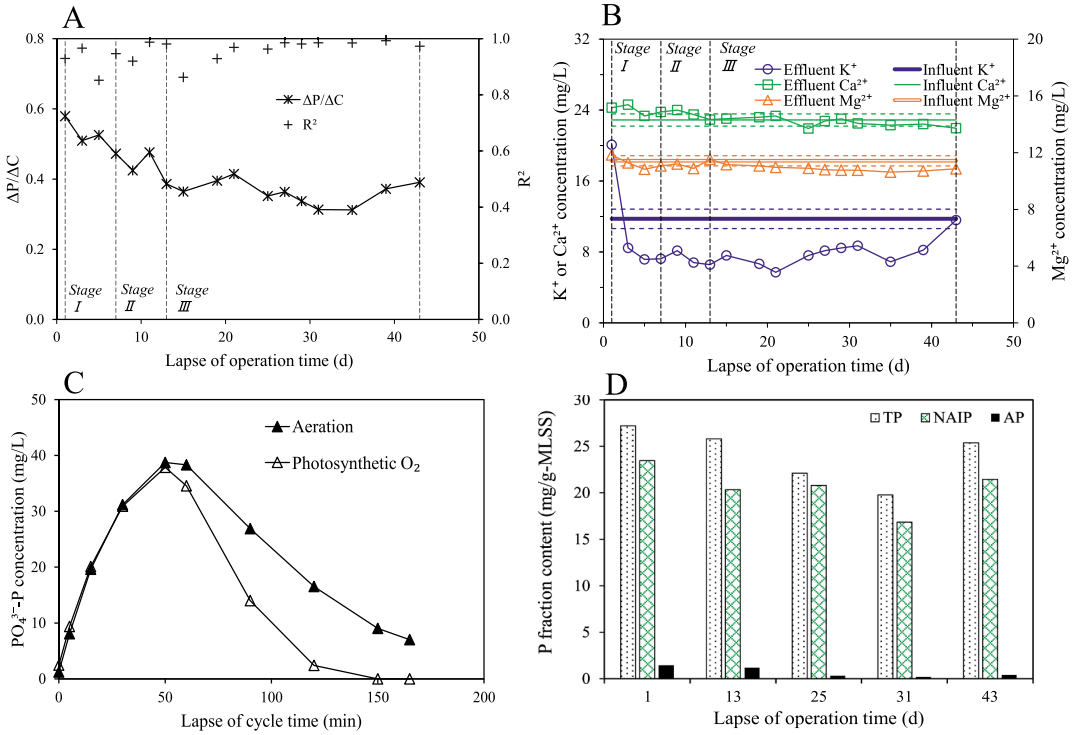

Fig. 7. Changes in molar ΔP/ΔC ratio and correlation coefficient (R^2) of ΔP against ΔC (A) and changes in effluent K^+, Mg^{2+} and Ca^{2+} concentrations (B) during the three operational stages; P profiles during the cycle tests using photosynthesis (Stage III) and mechanical aeration to supply O_2 (C); and changes in P fractionation in the granules during the test period (D).

K^+ and Mg^{2+} as the counterions of PO_4^{3-} are known to participate in anaerobic hydrolysis and aerobic synthesis of polyP at an assumed stoichiometry of $(K_{0.33}Mg_{0.33}PO_3)_n$. The increase in phototrophs abundance may change their quantitative relationship. From the cycle tests, the molar ΔK/ΔP and ΔMg/ΔP ratios were relatively stable (Fig. 7B), averagely 0.23 ± 0.02 and 0.28 ± 0.03, lower than the theoretical value of 0.33. This observation may support P assimilation by phototrophic organisms that result in low ΔK/ΔP and ΔMg/ΔP ratios. According to the TP removal efficiency and the assumed stoichiometry of polyP, the maximum contributions of PAOs to K^+ and Mg^{2+} reduction can be up to 7% and 4%, respectively. The latter estimation is close to the measured Mg^{2+} reduction, about 4 ± 2%, except on day 1 (Fig. 7B), but the former significantly deviated from the measured K^+ reduction (24 ± 11%) except on day 1. Such a deviation is probably associated with active assimilation by phototrophic organisms that require more K^+, which needs further confirmation. In the case of Ca^{2+}, besides the low pH condition, its negligible reduction in concentration may exclude Ca-P precipitation from the P removal pathway.

Fig. 7C presents the apparent advantage of the photosynthetic O_2 on P removal compared to the mechanical aeration due to a higher P uptake rate detected in the former. However, similar molar ratios under the two O_2 supply strategies did not support the phototrophs' P assimilation. A previous study found that microalgal P assimilation during aerobic P uptake from the liquid was negligible in the algal-bacterial AGS system; P for microalgae growth was from the solid (granules) instead of the liquid (Li et al., 2022). Generally, P assimilation by phototrophs requires a long HRT. The adopted short HRT of 6 h during Stage III in the present study may not highlight the contribution of assimilation. As shown in Table 2, according to the estimated contribution (0.60 mg/(g-MLSS•d)) of phototrophs to P assimilation, namely 0.1 mg/g-MLSS is required for each cycle. This value is significantly lower than the anaerobically released P (5.9 ± 1.1 mg/g-MLSS based on MLSS concentration during the last 12 days' operation). This study determined the P assimilation rate as 2.08 mg/(g-MLSS•d), mainly attributable to PAOs. As noted in

Table 2, the measured output TP cannot cover the input TP, probably due to TP dissolution from the effluent biomass during the collection and storage stages (for final determination).

3.6. Energy consumption and implications

The energy requirement by the biological treatment (especially the aeration unit) generally accounts for 50 – 70% of the total operating costs in WWTPs (Vergara-Araya et al., 2021). According to the ideal mixing energy requirement of 1.5 W/m^3 and the mixing energy of 5 W/m^3 in an example WWTP (Vergara-Araya et al., 2021), the energy consumption for only mixing applied in this study was about 5.75 Wh/m^3 during the oxic phase, significantly lower than 180–800 Wh/m^3 for the commonly mechanical aeration operation (Silva and Rosa, 2021). This observation implies that only mixing instead of mechanical aeration to suspend algal-bacterial granules is economically feasible. However, the energy consumption by stirring should be carefully re-examined when the reactor system is scaled up since the energy consumption may not increase linearly with the increase in system treatment capacity. On the other hand, a high electricity consumption of 36.73 kWh/m^3 for the LED lights is required (Supplementary Material), which can be replaced by natural sunlight and designed correspondingly in the followed-up research works.

The algal-bacterial AGS system is promising for C fixation and CO_2 emission reduction from WWTPs, which successfully assimilated 52% of the total input C. The fixed C estimated by the assumed formula of phototrophs Table 2) can be used to produce a maximum 55 mg-O_2 per cycle, enough to complete the high O_2 requirement by the nitrification process (35 mg-O_2, assimilated N was not counted) and aerobic P uptake process (15 mg-O_2) according to Eqs. (2) and ((3) and nutrient removal performance. This observation indicates that a higher C fixation could be achieved when treating wastewater with a higher NH_4^+-N concentration that requires more O_2. In addition, the DO control by switching on/off the light reduces illumination time from 115 min to 80 – 104 min, saving 10 – 30% of light energy requirement. As noted, compared to the energy-intensive mechanical aeration, the photosynthetic O_2 is more efficient for nutrients removal as the O_2 molecules generated by the coexisting microalgae inside or on the granule surface may avoid the resistance to gas diffusion and transfer from the gas phase to liquid phase and then into the granules.

4. Conclusions

The feasibility of using photosynthetic O_2 from phototrophic organisms for simultaneous aerobic nitrification and P uptake by PAOs in an algal-bacterial AGS system has been demonstrated. The energy consumption of 5.75 Wh/m^3 for mixing required only for the proposed system is more economical than that of mechanical aeration commonly used for AGS systems. Although the additional illumination cost by artificial lights was relatively high in this study, the DO control strategy involving switching the lights on and off could reduce light energy consumption by 10 – 30%.

In a short HRT of 6 h, the coexisting phototrophic organisms in algal-bacterial AGS could photosynthesize enough O_2 production to implement nitrification and aerobic P uptake. The system achieved a highly efficient TN removal of 81 ± 7% with an N assimilation rate of 7.55 mg/(g-MLVSS•d), mainly due to microbial assimilation and simultaneous nitrification/denitrification under the test conditions. In the proposed pH/DO- controlled algal-bacterial AGS system, PAOs dominated P removal process and exhibited high activity, as indicated by a high P release rate of 10.84 ± 0.41 mg/(g-MLVSS•h), P uptake rate of 7.18 ± 0.24 mg/(g-MLVSS•h), and a molar ΔP/ΔC ratio of 0.36 ± 0.03, resulting in TP removal greater than 92%.

Considering the scale-up and better O&M of the proposed algal-bacterial AGS system, a more in-depth research is demanded. C/N/P assimilation and removal mechanisms, contributions of microalgae/phototrophs and bacteria, light system design, the sensitivity of CO_2 emission to DO/pH control range, and influence of influent characteristics should be further explored during the long-term operation of the algal-bacterial AGS system.

CRediT authorship contribution statement

Zejiao Li: Conceptualization, Data curation, Formal analysis, Investigation, Methodology, Writing – original draft, Writing – review & editing. **Jixiang Wang:** Conceptualization, Data curation, Formal analysis, Investigation, Methodology, Writing – original draft, Writing – review & editing. **Jialin Liu:** Data curation, Methodology. **Xingyu Chen:** Data curation, Methodology. **Zhongfang Lei:** Conceptualization, Formal analysis, Funding acquisition, Project administration, Supervision, Writing – review & editing. **Tian Yuan:** Formal analysis, Methodology, Supervision. **Kazuya Shimizu:** Formal analysis, Methodology. **Zhenya Zhang:** Formal analysis, Methodology, Supervision. **Duu-Jong Lee:** Formal analysis, Methodology, Writing – review & editing. **Yuemei Lin:** Formal analysis, Writing – review & editing. **Yasuhisa Adachi:** Formal analysis, Methodology, Supervision. **Mark C.M. van Loosdrecht:** Formal analysis, Methodology, Writing – review & editing.

Declaration of Competing Interest

The authors declare that they have no known competing financial interests or personal relationships that could have appeared to influence the work reported in this paper.

Data availability

Data will be made available on request.

Acknowledgments

This work was supported by JSPS KAKENHI Grant Numbers JP22K19863 and JP22H00387, and JST Next Generation Researchers Challenging Research Program (No. JPMJSP2124) at University of Tsukuba, Japan.

Supplementary materials

Supplementary material associated with this article can be found, in the online version, at doi:10.1016/j.watres.2023.120025.

References

Abouhend, A.S., Gikonyo, J.G., Patton, M., Butler, C.S., Tobiason, J., Park, C., 2023. Role of hydrodynamic shear in the oxygenic photogranule (OPG) wastewater treatment process. ACS EST Water 3, 659–668. https://doi.org/10.1021/acsestwater.2c00317.

Abouhend, A.S., McNair, A., Kuo-Dahab, W.C., Watt, C., Butler, C.S., Milferstedt, K., Hamelin, J., Seo, J., Gikonyo, G.J., El-Moselhy, K.M., Park, C., 2018. The oxygenic photogranule process for aeration-free wastewater treatment. Environ. Sci. Technol. 52, 3503–3511. https://doi.org/10.1021/acs.est.8b00403.

Acevedo, B., Oehmen, A., Carvalho, G., Seco, A., Borrás, L., Barat, R., 2012. Metabolic shift of polyphosphate-accumulating organisms with different levels of polyphosphate storage. Water Res. 46, 1889–1900. https://doi.org/10.1016/J.WATRES.2012.01.003.

Adav, S.S., Lee, D.J., Show, K.Y., Tay, J.H., 2008. Aerobic granular sludge: recent advances. Biotechnol. Adv. 26, 411–423. https://doi.org/10.1016/j.biotechadv.2008.05.002.

APHA, 2012. Standard Methods for the Examination of Water and Wastewater. American Public Health Association/American Water Work Association/Water Environment Federation, Washington, D.C., USA.

Bao, Z., Sun, S., Sun, D., 2015. Characteristics of direct CO_2 emissions in four full-scale wastewater treatment plants. Desalin. Water Treat. 54, 1070–1079. https://doi.org/10.1080/19443994.2014.940389.

Boelee, N.C., Temmink, H., Janssen, M., Buisman, C.J.N., Wijffels, R.H., 2014. Balancing the organic load and light supply in symbiotic microalgal-bacterial biofilm reactors treating synthetic municipal wastewater. Ecol. Eng. 64, 213–221. https://doi.org/10.1016/j.ecoleng.2013.12.035.

Campos, J.L., Valenzuela-Heredia, D., Pedrouso, A., Val Del Río, A., Belmonte, M., Mosquera-Corral, A., 2016. Greenhouse gases emissions from wastewater treatment plants: minimization, treatment, and prevention. J. Chem., 3796352 https://doi.org/10.1155/2016/3796352, 2016.

Carvalheira, M., Oehmen, A., Carvalho, G., Eusébio, M., Reis, M.A.M., 2014. The impact of aeration on the competition between polyphosphate accumulating organisms and glycogen accumulating organisms. Water Res. 66, 296–307. https://doi.org/10.1016/j.watres.2014.08.033.

Chen, M., Oshita, K., Mahzoun, Y., Takaoka, M., Fukutani, S., Shiota, K., 2021. Survey of elemental composition in dewatered sludge in Japan. Sci. Total Environ. 752, 141857 https://doi.org/10.1016/j.scitotenv.2020.141857.

de Sousa Rollemberg, S.L., Mendes Barros, A.R., Firmino, P.I.M., Bezerra dos Santos, A., 2018. Aerobic granular sludge: cultivation parameters and removal mechanisms. Bioresour. Technol. 270, 678–688. https://doi.org/10.1016/j.biortech.2018.08.130.

Gerardi, M.H., 2002. Nitrification and Denitrification in the Activated Sludge Process, 1st ed. John Wily & Sons, Inc., New York.

Gonçalves, A.L., Pires, J.C.M., Simões, M., 2017. A review on the use of microalgal consortia for wastewater treatment. Algal Res. 24, 403–415. https://doi.org/10.1016/j.algal.2016.11.008.

He, Q., Chen, L., Zhang, S., Chen, R., Wang, H., Zhang, W., Song, J., 2018a. Natural sunlight induced rapid formation of water-born algal-bacterial granules in an aerobic bacterial granular photo-sequencing batch reactor. J. Hazard. Mater. 359, 222–230. https://doi.org/10.1016/j.jhazmat.2018.07.051.

He, Q., Chen, L., Zhang, S., Wang, L., Liang, J., Xia, W., Wang, H., Zhou, J., 2018b. Simultaneous nitrification, denitrification and phosphorus removal in aerobic granular sequencing batch reactors with high aeration intensity: impact of aeration time. Bioresour. Technol. 263, 214–222. https://doi.org/10.1016/j.biortech.2018.05.007.

He, Q., Zhang, S., Zou, Z., Zheng, L., Wang, H., 2016. Unraveling characteristics of simultaneous nitrification, denitrification and phosphorus removal (SNDPR) in an aerobic granular sequencing batch reactor. Bioresour. Technol. 220, 651–655. https://doi.org/10.1016/j.biortech.2016.08.105.

Huang, W., Li, B., Zhang, C., Zhang, Z., Lei, Z., Lu, B., Zhou, B., 2015. Effect of algae growth on aerobic granulation and nutrients removal from synthetic wastewater by using sequencing batch reactors. Bioresour. Technol. 179, 187–192. https://doi.org/10.1016/j.biortech.2014.12.024.

Ji, B., Liu, C., 2022. CO_2 improves the microalgal-bacterial granular sludge towards carbon-negative wastewater treatment. Water Res. 208, 117865 https://doi.org/10.1016/j.watres.2021.117865.

Ji, B., Zhang, M., Gu, J., Ma, Y., Liu, Y., 2020a. A self-sustaining synergetic microalgal-bacterial granular sludge process towards energy-efficient and environmentally sustainable municipal wastewater treatment. Water Res. 179, 115884 https://doi.org/10.1016/j.watres.2020.115884.

Ji, B., Zhang, M., Wang, L., Wang, S., Liu, Y., 2020b. Removal mechanisms of phosphorus in non-aerated microalgal-bacterial granular sludge process. Bioresour. Technol. 312, 123531 https://doi.org/10.1016/j.biortech.2020.123531.

Jones, E.R., Van Vliet, M.T.H., Qadir, M., Bierkens, M.F.P., 2021. Country-level and gridded estimates of wastewater production, collection, treatment and reuse. Earth Syst. Sci. Data 13, 237–254. https://doi.org/10.5194/essd-13-237-2021.

Larsen, T.A., 2015. CO_2-neutral wastewater treatment plants or robust, climate-friendly wastewater management? A systems perspective. Water Res. 87, 513–521. https://doi.org/10.1016/j.watres.2015.06.006.

Li, Z., Wang, J., Chen, X., Lei, Z., Yuan, T., Shimizu, K., Zhang, Z., Lee, D.J., 2022. Insight into aerobic phosphorus removal from wastewater in algal-bacterial aerobic granular sludge system. Bioresour. Technol. 352, 127104 https://doi.org/10.1016/j.biortech.2022.127104.

Liu, L., Fan, H., Liu, Y., Liu, C., Huang, X., 2017. Development of algae-bacteria granular consortia in photo-sequencing batch reactor. Bioresour. Technol. 232, 64–71. https://doi.org/10.1016/j.biortech.2017.02.025.

Luo, J., Hao, T., Wei, L., Mackey, H.R., Lin, Z., Chen, G.H., 2014. Impact of influent COD/N ratio on disintegration of aerobic granular sludge. Water Res. 62, 127–135. https://doi.org/10.1016/j.watres.2014.05.037.

Mosquera-Corral, A., De Kreuk, M.K., Heijnen, J.J., van Loosdrecht, M.C.M., 2005. Effects of oxygen concentration on N-removal in an aerobic granular sludge reactor. Water Res. 39, 2676–2686. https://doi.org/10.1016/j.watres.2005.04.065.

Muñoz, R., Guieysse, B., 2006. Algal-bacterial processes for the treatment of hazardous contaminants: a review. Water Res. 40, 2799–2815. https://doi.org/10.1016/j.watres.2006.06.011.

Nereda, 2023. https://nereda.royalhaskoningdhv.com/. Accessed on Jan. 2, 2023.

Oehmen, A., Lemos, P.C., Carvalho, G., Yuan, Z., Keller, J., Blackall, L.L., Reis, M.A.M., 2007. Advances in enhanced biological phosphorus removal: from micro to macro scale. Water Res. 41, 2271–2300. https://doi.org/10.1016/j.watres.2007.02.030.

Pancha, I., Chokshi, K., George, B., Ghosh, T., Paliwal, C., Maurya, R., Mishra, S., 2014. Nitrogen stress triggered biochemical and morphological changes in the microalgae Scenedesmus sp. CCNM 1077. Bioresour. Technol. 156, 146–154. https://doi.org/10.1016/j.biortech.2014.01.025.

Rajta, A., Bhatia, R., Setia, H., Pathania, P., 2020. Role of heterotrophic aerobic denitrifying bacteria in nitrate removal from wastewater. J. Appl. Microbiol. 128, 1261–1278. https://doi.org/10.1111/jam.14476.

Samiotis, G., Stamatakis, K., Amanatidou, E., 2021. Assessment of Synechococcus elongatus PCC 7942 as an option for sustainable wastewater treatment. Water Sci. Technol. 84, 1438–1451. https://doi.org/10.2166/wst.2021.319.

Silva, C., Rosa, M.J., 2021. A practical methodology for forecasting the impact of changes in influent loads and discharge consents on average energy consumption and sludge production by activated sludge wastewater treatment. Sustainability 13 (21), 12293. https://doi.org/10.3390/su132112293.

Slade, A.H., Anderson, S.M., Evans, B.G., 2003. Nitrogen fixation in the activated sludge treatment of thermomechanical pulping wastewater: effect of dissolved oxygen. Water Sci. Technol. 48, 1–8. https://doi.org/10.2166/wst.2003.0446.

Smolders, G.J.F., van Loosdrecht, M.C.M., Heijnen, J.J., 1995. A metabolic model for the biological phosphorus removal process. Water Sci. Technol. 31, 79–93. https://doi.org/10.2166/WST.1995.0078.

Sousa, C., Compadre, A., Vermuë, M.H., Wijffels, R.H., 2013. Effect of oxygen at low and high light intensities on the growth of Neochloris oleoabundans. Algal Res. 2, 122–126. https://doi.org/10.1016/j.algal.2013.01.007.

Vergara-Araya, M., Hilgenfeldt, V., Peng, D., Steinmetz, H., Wiese, J., 2021. Modelling to lower energy consumption in a large WWTP in China while optimising nitrogen removal. Energies 14 (18), 5826. https://doi.org/10.3390/en14185826.

Wang, J., Lei, Z., Tian, C., Liu, S., Wang, Q., Shimizu, K., Zhang, Z., Adachi, Y., Lee, D.J., 2021. Ionic response of algal-bacterial granular sludge system during biological phosphorus removal from wastewater. Chemosphere 264, 128534. https://doi.org/10.1016/j.chemosphere.2020.128534.

Wang, J., Lei, Z., Wei, Y., Wang, Q., Tian, C., Shimizu, K., Zhang, Z., Adachi, Y., Lee, D.J., 2020. Behavior of algal-bacterial granular sludge in a novel closed photo-sequencing batch reactor under no external O_2 supply. Bioresour. Technol. 318, 124190 https://doi.org/10.1016/j.biortech.2020.124190.

Wang, J., Wei, Y., Li, Z., Chen, X., Lei, Z., Yuan, T., Shimizu, K., Zhang, Z., Kim, S.H., Lee, D.J., 2022. Effect of stepwise or one-time illumination strategy on the development of algal-bacterial aerobic granular sludge in sequencing batch reactor. Bioresour. Technol. Rep. 17, 100931 https://doi.org/10.1016/j.biteb.2021.100931.

Wang, Q., Shen, Q., Wang, J., Zhang, Y., Zhang, Z., Lei, Z., Shimizu, K., Lee, D.J., 2020. Fast cultivation and harvesting of oil-producing microalgae Ankistrodesmus falcatus var. acicularis fed with anaerobic digestion liquor via biogranulation in addition to nutrients removal. Sci. Total Environ. 741, 140183 https://doi.org/10.1016/j.scitotenv.2020.140183.

Zhang, H., Gong, W., Bai, L., Chen, R., Zeng, W., Yan, Z., Li, G., Liang, H., 2020. Aeration-induced CO_2 stripping, instead of high dissolved oxygen, have a negative impact on algae–bacteria symbiosis (ABS) system stability and wastewater treatment efficiency. Chem. Eng. J. 382, 122957 https://doi.org/10.1016/j.cej.2019.122957.

Zhao, Z., Liu, S., Yang, X., Lei, Z., Shimizu, K., Zhang, Z., Lee, D.J., Adachi, Y., 2019. Stability and performance of algal-bacterial granular sludge in shaking photo-sequencing batch reactors with special focus on phosphorus accumulation. Bioresour. Technol. 280, 497–501. https://doi.org/10.1016/j.biortech.2019.02.071.

Zhao, Z., Yang, X., Cai, W., Lei, Z., Shimizu, K., Zhang, Z., Utsumi, M., Lee, D.J., 2018. Response of algal-bacterial granular system to low carbon wastewater: focus on granular stability, nutrients removal and accumulation. Bioresour. Technol. 268, 221–229. https://doi.org/10.1016/j.biortech.2018.07.114.